Supplemental data

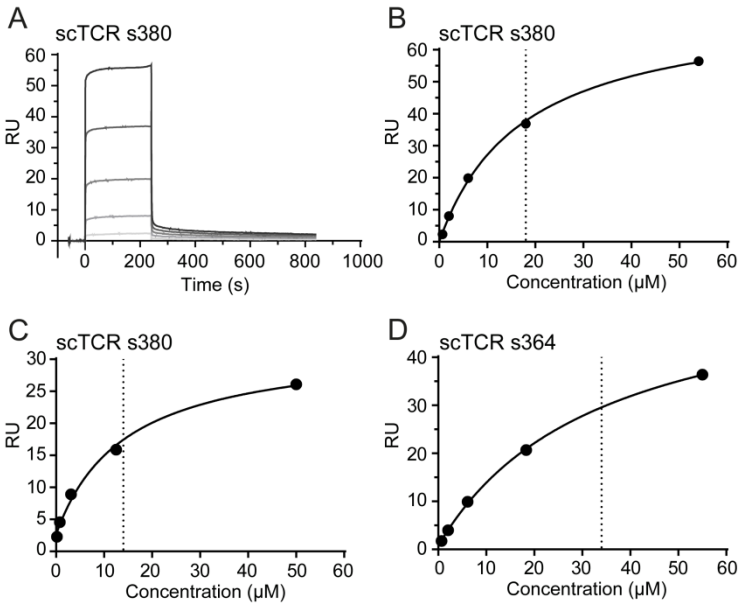

Figure S1. Surface Plasmon Resonance (SPR) data of single chain T-cell receptor (scTCR) s380 and s364 binding to DQ2.5:DQ2.5-glia-α1a and DQ2.5:DQ2.5-glia-α2, respectively. (**A**) Representative sensogram of scTCR s380 binding to immobilized DQ2.5:DQ2.5-glia-α1a using a classical multi-cycle kinetic SPR setup. The affinity was determined by fitting the data to a 1:1 Langmuir binding model. (**B**) Equilibrium dissociation constant (K_D) was determined by plotting the response at equilibrium from (A) against the concentration of analyte (scTCR s380). (**C and D**) The equilibrium responses of the single-cycle kinetics data in Figure 1C and D plotted against the concentration of (C) scTCR s380, and (D) scTCR s364 to derive the equilibrium dissociation constant (K_D). Dotted line indicates the K_D based on fitting the response to saturation. The K_D values are summarised in Table S1.

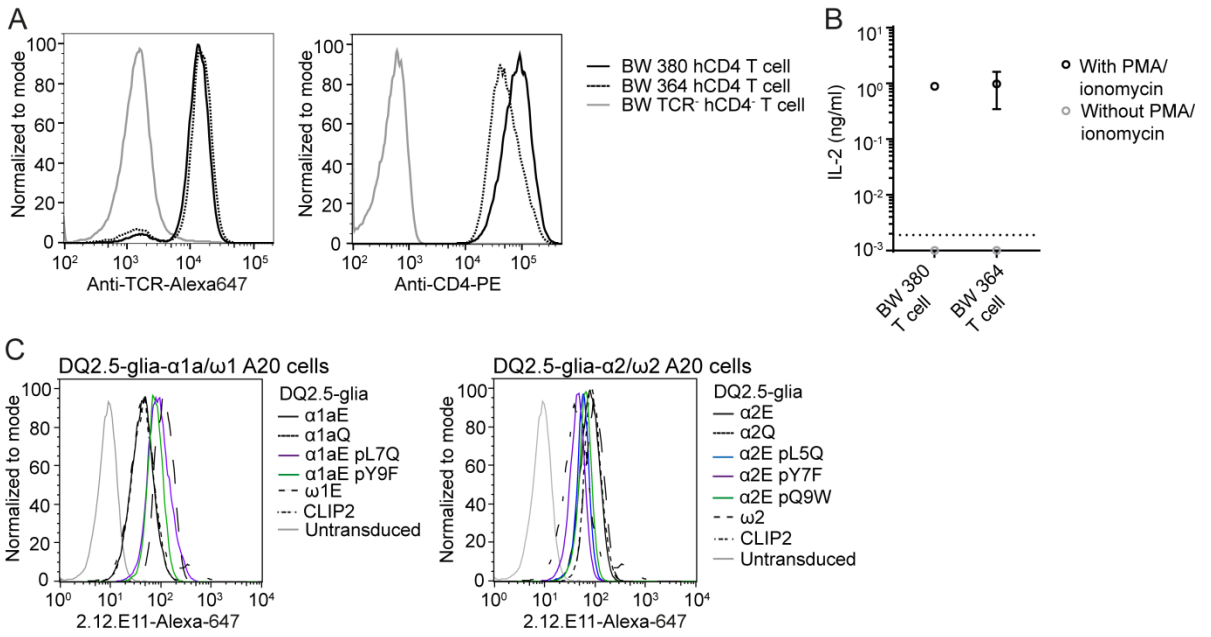

Figure S2. Validation of T-cell receptor (TCR), CD4 and HLA-DQ2.5-peptide expression levels and stimulatory capacity of the BW 380 and 364 T cells. (**A**) BW 380 and 364 T cells stained with either anti-TCR-Alexa 647 or anti-CD4-PE mAbs were analyzed by flow cytometry to validate the TCR and CD4 expression levels. Untransduced BW T cells devoid of endogenous TCR and human CD4 were used as control. (**B**) The BW 380 and 364 T cells were stimulated with a PMA/ionomycin followed by measurement of IL-2 secretion to assess their stimulatory capacity. The dotted line indicates the detection limit, and error bars indicate ± SD of triplicates and are only shown if they exceed the size of the symbol. (**C**) HLA-DQ2.5-peptide expression levels on the A20 cells transfected with HLA-DQ2.5 with covalently linked peptide was assessed in flow cytometry after staining with the biotinylated mAb 2.12.E11 specific for HLA-DQ2 β-chain, followed by streptavidin Alexa-647. Untransduced A20 cells devoid of HLA were used as control. (**A-C**) Two (A and C) or three (B) independent experiments were conducted. **(B)** Figures were prepared using GraphPad Prism 7. Non-linear regression analysis (three parameters) was used to derive IL-2 concentrations from the standard curves.

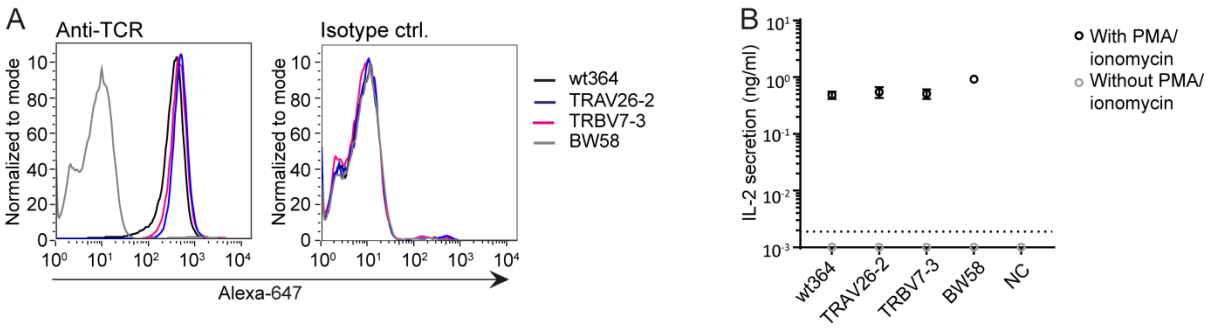

Figure S3. T-cell receptor (TCR) expression level and stimulatory capacity of the BW 364 T cells and the BW 364 T cell variants. The *TRAV* and *TRBV* BW T cell exchange mutants were evaluated by (**A**) staining with anti-TCR-Alexa-647 mAb, or isotype control, followed by analysis by flow cytometry to validate TCR expression levels, and (**B**) stimulation with a PMA/ionomycin cocktail followed by measurement of IL-2 secretion to assess equal stimulatory capacity. The dotted line indicates the detection limit, and error bars indicate ± SD of triplicates and are only shown if they exceed the size of the symbol. (**A-B**) Two (A) or four (B) independent experiments were conducted. **(B)** Figures were prepared using GraphPad Prism 7. Non-linear regression analysis (three parameters) was used to derive IL-2 concentrations from the standard curves.

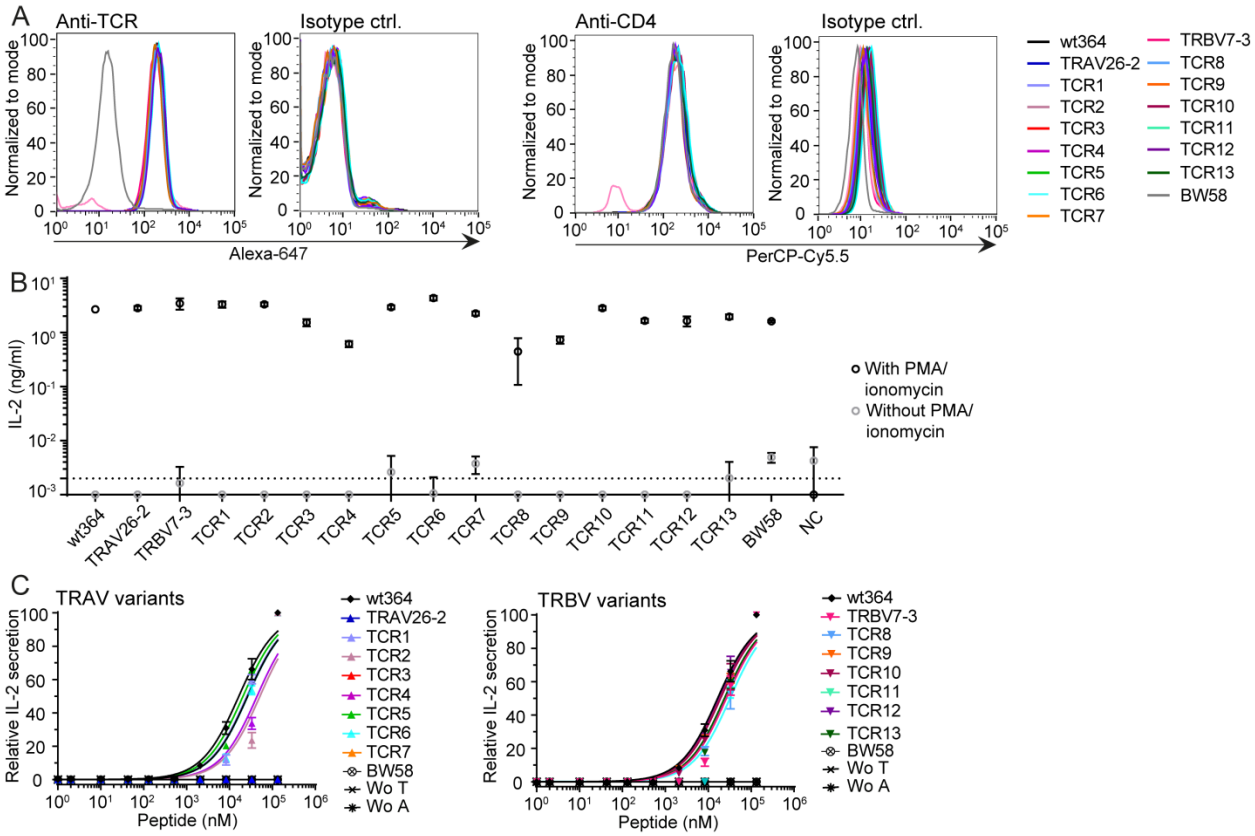

Figure S4. T-cell receptor (TCR) and CD4 expression levels and stimulatory capacity of the BW 364 T cell variants. All *TRAV* and *TRBV* mutant variants used to assess the contribution of germline variants were evaluated by (**A**) staining with anti-TCR-Alexa-647, anti-CD4-PerCP-Cy5.5, or isotype controls, followed by flow cytometry, and (**B**) stimulation with a PMA/ionomycin cocktail followed by measurement of IL-2 secretion. The dotted line indicates the detection limit, and error bars indicate ± SD of triplicates and are only shown if they exceed the size of the symbol. (**C**) HLA-DQ2.5^{+} EBV-B cells were loaded with native 33merQ peptide and IL-2 secretion level determined by ELISA. Error bars indicate ± SD of triplicates. (**A-C**) Two (A) or four (B and C) independent experiments were conducted. **(B and C)** Figures were prepared using GraphPad Prism 7. Non-linear regression analysis (three parameters) was used to derive IL-2 concentrations from the standard curves.

Table S1. SPR data of scTCRs s380 and s364

TCR clone	Method	K_D (kd/ka)	K_D (eq.)	Average K_D
380	SCK[A]	7.9	14.3	11.1
380	SCK[A]	21.6	24.5	23.1
380	MCK[B]	15.1	17.5	16.3
380				17[C]
364	SCK[A]	47.6	42.3	45.0
364	SCK[A]	31.3	33.9	32.6
364	SCK[A]	35.4	NA	NA
364				38[C]

[A] SCK; single-cycle kinetics
[B] Classical MCK; multi-cycle kinetics
[C] Average K_D value based on values derived from both the affinity constant (kd/ka) and the equilibrium dissociation constant.

Table S2. Sequence alignment of *TRAV26-1* and other *TRAVs* paired with the canonical CDR3β in CD patients.

V-gene[A] IMGT no.	FR1 1 ----------→26	CDR1 27-------→38	FR2 39----------→55	CDR2 56----→65	FR3 66 ----------→104
TRAV26-1	DAKTTQ.PPSMDCAE GRAANLPCNHS	TISG.....NE**Y**	V**Y**WYRQIH SQGPQYII**H**	GLK.....NN	ETNE…MASLIITEDR KSSTLILPHATL RDTAVYYC
TRAV5	GEDVEQS.LFLSVRE GDSSVIN**C**TYT	DSS.....ST**Y**	L**Y**WYKQEP GAGLQLLT**Y**	IFSN...MDM	KQD.....Q RLTVLLNKKD KHLS**L**RIADTQT GDSAIYF**C** AES
TRAV39	ELKVEQNPLFLSMQE GKNYTIY**C**NYS	TTS.....D**R**	L**Y**WYRQDP GKSLESLF**V**	LLSN...GAV	KQE.....G RLMASLDTKA RLST**L**HITAAVH DLSATYF**C** AVD
TRAV8-6	AQSVTQLDSQVPVFE EAPVELR**C**NYS	SSV.....SV**Y**	L**F**WYVQYP NQGLQLLL**K**	YLSG..STLV	ESI.....N GFEAEFNKSQ TSFH**L**RKPSVHI SDTAEYF**C**
TRAV38-1	AQTVTQSQPEMSVQE AETVTLSCTYD	TSEN.....NY**Y**	L**F**WYKQPP SRQMILVI**R**	QEAY..KQQN	ATE.....N RFSVNFQKAA KSFSLKISDSQL GDTAMYFC
TRAV29[B]	DQQVKQNSPSLSVQE GRISILNCDYT	NSM.....FD**Y**	FLWYKKYP AEGPTFLI**S**	ISSI...KDK	NED.....G RFTVFLNKSA KHLSLHIVPSQP GDSAVYFC
TRAV13-2	GESVGLHLPTLSVQE GDNSIINCAYS	NSA.....SD**Y**	FIWYKQES GKGPQFII**D**	IRSN...MDK	RQG.....Q RVTVLLNKTV KHLSLQIAATQP GDSAVYFC
TRAV12-3	QKEVEQDPGPLSVPE GAIVSLNCTYS	NSA.....FQ**Y**	F**M**WYRQYS RKGPELLM**Y**	TYS....SGN	KED.....G RFTAQVDKSS KYISLFIRDSQP SDSATYLC

[A] *TRAV* gene segment usage and numbering was defined by the IMGT Database.
[B] *TRAV29/DV5*
Amino acids in position 38, 40 and 55 are indicated in bold and red characters.

Table S3. Gene segment usage and CDR3 sequences of the clones

Clone	*TRAV*	CDR3	*TRAJ*	*TRBV*	CDR3	*TRBJ*
380	*TRAV9-2*	ALSDHYSSGSARQLT	*TRAJ22*	*TRBV7-2*	ASSTAVLAGGPQY	*TRBJ2-7*
364	*TRAV26-1*	IVTNNNDMR	*TRAJ43*	*TRBV7-2*	ASSIRSTDTQY	*TRBJ2-3*
AV5BV7[A]	*TRAV5*	AESPGPGKLI	*TRAJ37*	*TRBV7-2*	ASSLRSADTQY	*TRBJ2-3*
AV39BV7[A]	*TRAV39*	AVDPP	*TRAJ43*	*TRBV7-3*	ASSFRSTDTQY	*TRBJ2-3*
AV8TV7[A]	*TRAV8-6*	AVTRNSGGYQKVT	*TRAJ13*	*TRBV7-2*	ASSIRSTDTQY	*TRBJ2-3*
AV38TV7[A]	*TRAV38-1*	APDPSTSGTYKYI	*TRAJ40*	*TRBV7-2*	ASSLRFTDTQY	*TRBJ2-3*
AV29TV7[A]	*TRAV29*[B]	AEGITGANSKLT	*TRAJ56*	*TRBV7-2*	ASSIRATDTQY	*TRBJ2-3*
AV13TV7[A]	*TRAV13-2*	AESGYSTLT	*TRAJ11*	*TRBV7-2*	ASSVRSTDTQY	*TRBJ2-3*
AV12TV7[A]	*TRAV12-3*	AMKEYGNKLV	*TRAJ47*	*TRBV7-2*	ASSLRSTDTQY	*TRBJ2-3*

TRAV gene segment usage and numbering was defined by the IMGT Database.
[A] Clonotypes identified by high-throughput sequencing
[B] *TRAV29/DV5*